

Environmental stress cracking of rubber-modified styrenic polymers in Freon vapour*

Kilwon Cho†, Min Soo Lee, and Chan Eon Park

Department of Chemical Engineering, Pohang University of Science and Technology, Pohang, 790-600 Korea

(Received 17 September 1996)

The effects of incorporation of rubber particles on the environmental stress cracking (ESC) behaviour of rubber modified polystyrene (PS) and styrene–acrylonitrile copolymer (SAN) in Freon vapour have been investigated in view of the rubbery particle size and rubber content. Core–shell particles such as poly(*n*-butyl acrylate) rubber core/PS or poly(methyl methacrylate) shell particles of 0.2–2 μm in rubbery core diameter were prepared, and these particles were incorporated into a PS or SAN matrix. The larger particles, about 1–2 μm , showed the higher ESC resistance for rubber modified PS, whereas for SAN alloys small particles around 300 nm were the most effective in ESC resistance. Microscopic examination on the Freon-exposed specimen surface revealed that the surface damage is well developed craze in homo PS, and the development of craze is suppressed with increasing rubber content. The yielded lines were observed in homo SAN, and they became vague and diffuse with increasing rubber content. From these results, it was concluded that the role of rubber particles in the ESC process of rubber modified styrenic polymers in Freon vapour is to promote surface plasticization and to suppress the development of local damage on the specimen surface.

© 1997 Elsevier Science Ltd.

(Keywords: environmental stress cracking; polystyrene; styrene-acrylonitrile copolymer)

INTRODUCTION

Environmental stress cracking or crazing (ESC) of polymers has been a serious problem in practical applications, because it causes severe mechanical damage and reduces the service life time of polymers.

In the ESC process, the critical stress for initiation of crazes or cracks decreases dramatically^{1–6}. Basically, ESC is a result of a combination of environmental agent and stress, i.e. result of enhanced craze or crack growth and breakdown under load and under the influence of an aggressive agent. The stress can be external stress caused by external loads or internal residual stress resulting from fabrication processes. As an ESC agent, organic fluid and organic vapour are known to be the most aggressive agents^{7–18}. Inert gases such as N₂, O₂, CO₂, and Ar are also proved to be harmful on thermoplastics near their boiling points^{19–23}.

ESC can be explained in terms of either plasticization theory or surface energy reduction mechanism. Based on plasticization theory^{9,16,24,25}, ESC occurs by the plasticization of a stress concentration point due to diffusion of small environmental molecules. Surface energy reduction theory suggests^{2,7,8} that ESC agents having a low surface tension adhere on a polymer surface and reduce the surface energy, which initiates crazing or cracking of the material easily. The degree of ESC was

found to be closely related to the solubility parameter difference between polymer and the ESC agent^{2,26}. According to that, the critical stress for the environmental crazing or cracking shows a minimum when the solubility parameter of the environmental agent matches that of the polymer^{27,28}.

Several approaches have been carried out to enhance ESC resistance such as increasing the molecular weight of polymers, decreasing the compatibility between polymers and the ESC agent by controlling the composition and microstructure of polymers, and reducing residual stress in processing, etc. One approach, rubber modification, has been known to be a very effective method to increase critical strain for craze or crack formation²⁶.

Considering the practical application of ESC resistant rubber modified styrenic polymers, high impact polystyrene (HIPS) and acrylonitrile butadiene styrene copolymer (ABS) are typical ones. HIPS and ABS are widely used in liners and inner doors of refrigerators. Freon is still the main foaming agent of polyurethane insulation in refrigerators. Thus, some possible absorption may occur during the manufacturing process, or in service, which sometimes causes severe mechanical damage on the liner or inner panel. Knowledge of failure behaviour in this environment is required. However, little work has been reported on the environmental effect of Freon vapour on styrenic polymers^{27–29}.

Works on ESC of rubber modified thermoplastics had been performed by Henry²⁶ and others^{4,10,13,30} in a liquid environment. They found that the critical strain for crazing increases significantly with the addition of rubber

* Dedicated to Professor Tae Oan Ahn on the occasion of his 65th Birthday

† To whom correspondence should be addressed

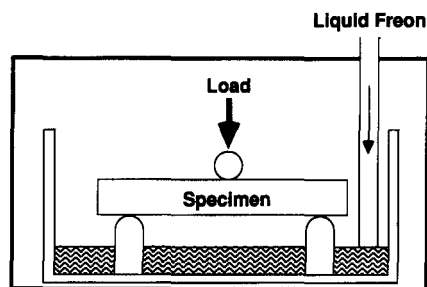


Figure 1 Schematic diagram of test device for craze or crack formation in Freon 11 vapour

particles. However, there are still so many open questions such as the role of rubber particles, rubber particle size effect, and the deformation mechanism, etc.

In this paper, a systematic model study has been carried out to understand the ESC behaviour of rubber modified styrenic polymers in a Freon vapour environment as a model study of HIPS and ABS. For this purpose, core-shell particles with uniform size were prepared by emulsion polymerization and these particles were incorporated into PS and SAN matrix as a simple model for HIPS and ABS. The effect of particle size, rubber phase content, and deformation mechanism have been investigated using bending tests and microscopic examination.

EXPERIMENTAL

Materials

PS and SAN as matrix materials were supplied by Cheil Industries. The \overline{M}_w of PS is $260\,000\text{ g mol}^{-1}$ ($\overline{M}_w/\overline{M}_n = 2.2$). The \overline{M}_w of SAN is $150\,000\text{ g mol}^{-1}$ ($\overline{M}_w/\overline{M}_n = 2.0$) and the acrylonitrile content is 28.5 wt%. The liquid Freon 11 (CFCl_3 , bp 23.7°C) was purchased from Ulsan Petrochemical Company.

Preparation of rubber particles and test specimens

The core-shell particles were prepared by sequential emulsion polymerization³¹. The rubbery core consists of poly(*n*-butyl acrylate) (PBA) and it was slightly cross-linked by 0.5 wt% of 1,4 butanediol diacrylate to retain its spherical morphology and size during melt blending with matrix materials and during subsequent moulding of the blends. The glass transition temperature (T_g) of the core material was about -40°C by dynamic mechanical measurements. As shell materials, slightly crosslinked PS and PMMA were used for PS and SAN matrix, respectively. PMMA is known to be compatible with SAN-28³². Good interfacial adhesion, therefore, is expected between the matrix SAN and the PMMA shell. The degree of crosslinking of the shell materials was minimized to be about 0.2 wt% of crosslinking agent to minimize the effect of rigid shell. PS and PMMA were crosslinked by divinyl benzene and 1,4 butandiol diacrylate, respectively. The composition ratio of rubbery core and glassy shell materials was 4/6 by weight.

The particle sizes and morphologies of the PBA-PS and PBA-PMMA core-shell particles were determined by scanning electron microscope (SEM) and transmission electron microscope (TEM). The size of rubbery core particles was varied from 0.2 to $2\ \mu\text{m}$. The shape of the rubbery core and core-shell particles was found to be quite spherical and the distribution of particle size was

relatively narrow. Two apparent loss peaks of PBA and PS were detected at -40°C and 105°C , respectively for synthesized PBA-PS core-shell particles by dynamic mechanical measurements. From these results it is believed that core-shell particles were well-produced and have uniform size. The prepared particles were isolated by filtration, washed thoroughly with distilled water and then dried at 50°C in vacuum for 1 week. The dried particles were blended with matrix materials in a melt blender (Brabender) for 10 min at 180°C . The blends were compression moulded into sheets of 6 mm thickness at 180°C for 10 min, and they were slowly cooled down to room temperature under low pressure to minimize residual stress. In the preliminary experiment, the moulded homoPS annealed at 110°C for 1 day did not show any marked difference in critical stress from the moulded specimen without annealing, so the annealing step was ignored. The test specimens of desired size ($6\text{ mm} \times 3\text{ mm} \times 60\text{ mm}$) were obtained by sawing and polishing of the sheet.

Determination of critical stress and relaxation experiment

The critical stress (σ_c) and strain (ϵ_c) at which craze or crack initiates on the specimen surface were determined by a three-point bending test (span 48 mm). The schematic diagram of the test device is shown in Figure 1. The test specimen was stressed to a fixed load value using a bending jig by universal testing machine (Instron 4206) in an environmental chamber. The chamber was maintained at 32°C , which is a sufficiently high temperature for evaporation of liquid Freon. After 1 min loading which is enough time to stabilize the loading condition, a large amount of liquid Freon was injected to the bottom of the chamber apart from the specimen. The liquid Freon was then vaporized rapidly, and the test specimen was surrounded by the Freon vapour. The Freon vapour pressure was believed to be saturated. After 1 min of exposure, the test specimen was taken out from the chamber and the specimen surface was examined by optical microscopy to see whether there was any damage. If crazes or cracks had not occurred on the surface of the specimen, the exposed specimen was discarded and a somewhat higher stress was applied to the new specimen. By the repeated procedure of this test, the values of critical stress or strain below which surface damage (crack or craze) could not be detected were determined.

Using this bending test, the stress relaxation behaviour of rubber-modified PS and SAN alloys was also investigated in Freon vapour. For PS alloys about 10 MPa stress was applied and for SAN alloys about 30 MPa stress was applied in the relaxation test. The applied stress was a little higher than the critical stress of the relevant homopolymer. Like the critical stress measurements, Freon was introduced in an environmental chamber after 1 min of loading. The relaxation of the stress was monitored for about 2–3 min after Freon exposure.

Microscopy and other tests

SEM observation was performed to examine surface damage developed by Freon vapour. For this purpose a thin sheet, of thickness 0.2 mm, was bent and fixed with a metal plate to keep the bending state. The specimen was exposed to Freon vapour in the environmental chamber, like the critical stress measurements. After exposure, the

specimen was dried in vacuum and the damaged zone was examined using SEM. Using this technique, it could be possible to examine the surface damage under stressed conditions.

To quantify the amount of the vapour absorption, a sheet of 2 mm thick was cut into strips of 10 mm × 50 mm. The test piece was placed in saturated Freon vapour at room temperature and the weight of specimen was measured with time. A creep device was used to verify the stress effect on absorption rate in that condition. In order to measure the T_g of Freon-invaded styrenic polymers, the dynamic mechanical measurements were carried out for the Freon-vapour-absorbed specimen using a dynamic mechanical thermal analyser (d.m.t.a., Polymer Laboratory MKII). The absorbed specimen was immediately clamped into the d.m.t.a. chamber, which had been already cooled to -100°C , to minimize the evaporation of Freon from the specimen.

RESULTS AND DISCUSSION

Surface damage of PS alloys

Above the critical stress, the development of damage lines on the specimen surface was almost simultaneous with exposure of Freon vapour. In optical microscopic observations of the damage on the specimen surface, the surface damage was changed from a narrow single straight line to a diffuse damage band in the PS matrix by the addition of rubber particles (*Figure 2*). At a low rubber content, only one or two damage lines were found around critical stress. The shape of the damage line for PS alloy containing 2 wt% rubber particles looks like a straight line (*Figure 2a*), and the damage line grew deep in the specimen surface. However, as the rubber content increases, the damage line becomes a zigzag feature, and has some tiny branches (*Figures 2b and 2c*). By the addition of 20 wt% of large size particles such as 1- μm particles, the narrow damage line was not detected, and only a diffuse damage band was suddenly developed above a critical stress (*Figure 2d*). The critical stress also jumped to high values at that rubber content. For small size particle inclusions, however, the damage lines did not exhibit such a broad band, even in the 20 wt% content (*Figure 2b*). The diffuse damage band observed at high rubber content and large rubber particles was quite different in shape with the narrow damage lines at low rubber content.

To make a more detailed examination on surface damages of PS alloy, SEM observation was carried out on the surface of the highly bent specimen containing large particles (*Figure 3*). By contrast to homoPS, of which the damage was a well-structured single craze (*Figure 3a*), the damage on the surface of the specimen containing 10 wt% rubber particles contains relatively short craze fibrils, and the fibril elongation seems to be much hindered (*Figure 3b*). For the specimen containing 20 wt% of large size particles, the broad damage lines shown in *Figure 2d* look like a bundle of small crazes near the critical stress. However, they do not have craze fibrils, i.e. a flock of concave lines (*Figure 3c*). When the applied stress is much above the critical stress, the broad damage was confirmed to be a flock of small crazes (*Figures 3d and 3e*). In that case, the crazes were spread broadly on the surface, rather than penetrating into the bulk. From this SEM observation, it is suggested that the

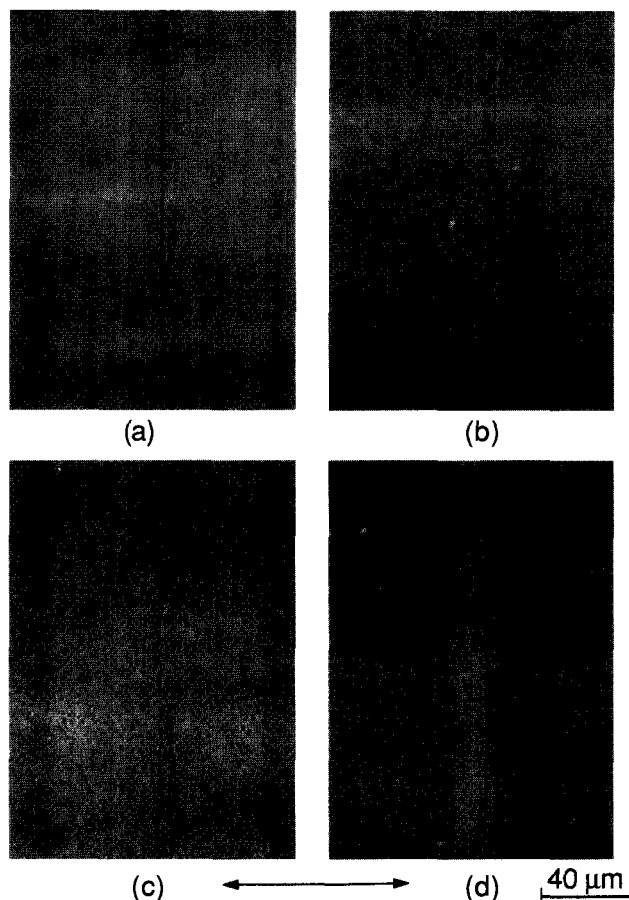


Figure 2 Optical micrographs of PS alloys showing surface damage by Freon vapour. (a) 300 nm, 2 wt%; (b) 300 nm, 20 wt%; (c) 1 μm , 15 wt%; (d) 1 μm , 20 wt%. (Particle size represents the diameter of rubbery core)

rubber particles suppress the development of well structured craze, and induce bundles of small crazes broadly on the surface region in PS matrix. This tendency becomes more apparent in larger particle inclusion. The higher stress is, therefore, needed to produce a flock of small size crazes over a relatively broad surface, which results in much increase of critical stress.

Surface damage of SAN alloys

Above the critical stress, the development of the damage line on the specimen surface of homoSAN was also simultaneous with exposure of Freon vapour like PS, although SAN is more resistant to Freon than PS²⁸. However, the shape of the damage line was rather short and dim compared with that of homoPS.

For SAN alloys, the surface damage by Freon exposure was not well detected using optical microscopy, because the damage was not clear. Therefore, SEM observation was performed on the highly bent specimen (*Figure 4*). In homoSAN, the damage lines were long yielded bands with no voids. However, the line does not seem to be a shear-yielded band, because the direction of the damage line was perpendicular to the applied stress. The damage lines become narrow and short with increasing rubber content. In the micrographs, many holes can be seen besides the damage lines on the rubber modified specimen surfaces (*Figure 4b*). The holes were the traces of rubber inclusions, which were influenced in

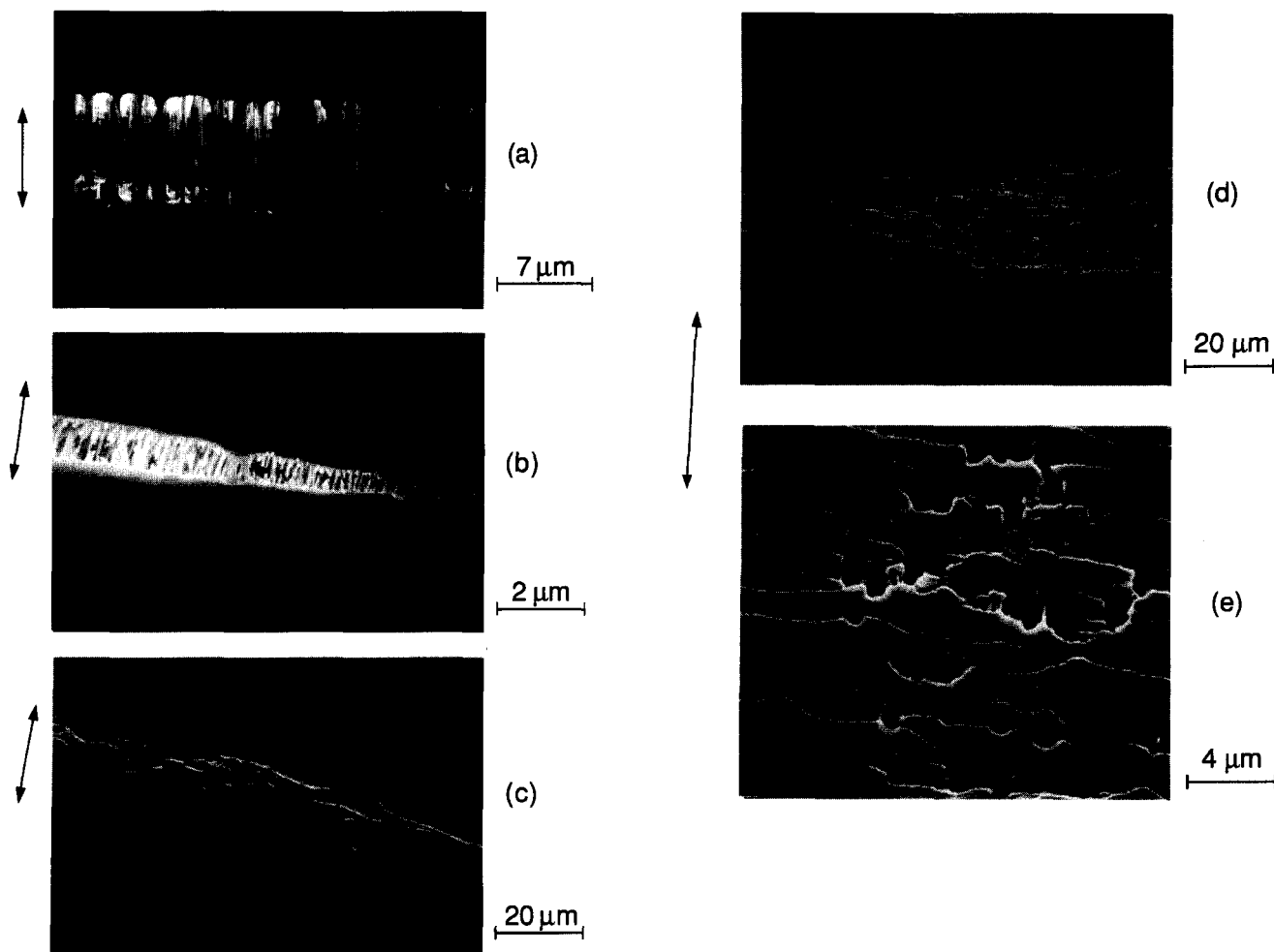


Figure 3 SEM micrographs of surface damage of PS alloy containing 2 μm PBA rubber particles. (a) 2 wt%; (b) 10 wt%; (c) 20 wt% rubber content, near critical stress; (d) 20 wt% rubber content, far above critical stress; (e) higher magnification of (d). Micrographs were taken under the bent state

their dimension by Freon vapour, since they could also be seen after Freon exposure in the case of unstressed conditions. Thus these holes were not considered as damage due to ESC. Therefore, the important damage is the band lines. At 20 wt% rubber content, the band lines disappeared and it was hard to detect damage lines (Figure 4c).

The Freon vapour did not induce well-developed crazes in SAN alloys. The damage lines did not propagate into the bulk and they were only placed on the surface region. This microscopic observation was in good agreement with SAN being more resistant to Freon vapour than PS, due to a larger difference in solubility parameter between Freon and SAN²⁸.

Critical stress and strain of PS alloys

It is known that the craze or crack development by an organic medium needs some induction time in the case of mild conditions^{7,16,30}. However, above the critical stress, the development of damage lines on the surface of PS alloys occurred almost simultaneously with exposure of Freon vapour, since Freon 11 is a very aggressive agent to PS. On the other hand, below the critical stress, only surface softening was observed instead of damage lines even for long exposure time. Therefore, 1 min was enough to cause damage on the surface of the specimen.

The variation of critical stress and critical strain at

which crazes start to form is plotted against the rubber content for PS alloys containing three different sizes of (PS-PBA) core-shell particles in Figure 5. It can be seen that the critical stress decreases as the rubber content increases until 15 wt%, and above that content the critical stress increases again, except for the 300 nm particle size, at which the critical stress stabilizes. This trend of increase of critical stress at high rubber content becomes more apparent at larger particle sizes.

The particle size effect becomes clear when the critical stress values are plotted for 20 wt% rubber content (Figure 6). At 300 nm particle size, the value of critical stress was slightly lower than that of homoPS. Above 600 nm the critical stress increased rapidly. From these results it seems that the rubber particle size of 1 μm is quite effective for improving the environmental stress cracking resistance to Freon vapour for PS alloy when the rubber content is relatively high, say 20 wt%.

However, when the rubber content is less than 15 wt%, the critical stress decreases with inclusion of rubber particles (Figure 5), i.e. ESC resistance of rubber-modified PS alloy containing a small amount of rubber particles becomes worse than homo PS. From the optical microscopic examination of the surface of the tested specimen, it was observed that the craze or crack is always initiated at the rubber inclusion site. This observation may be reasonable, because the applied stress is concentrated around a rubber particle. So it is considered that the

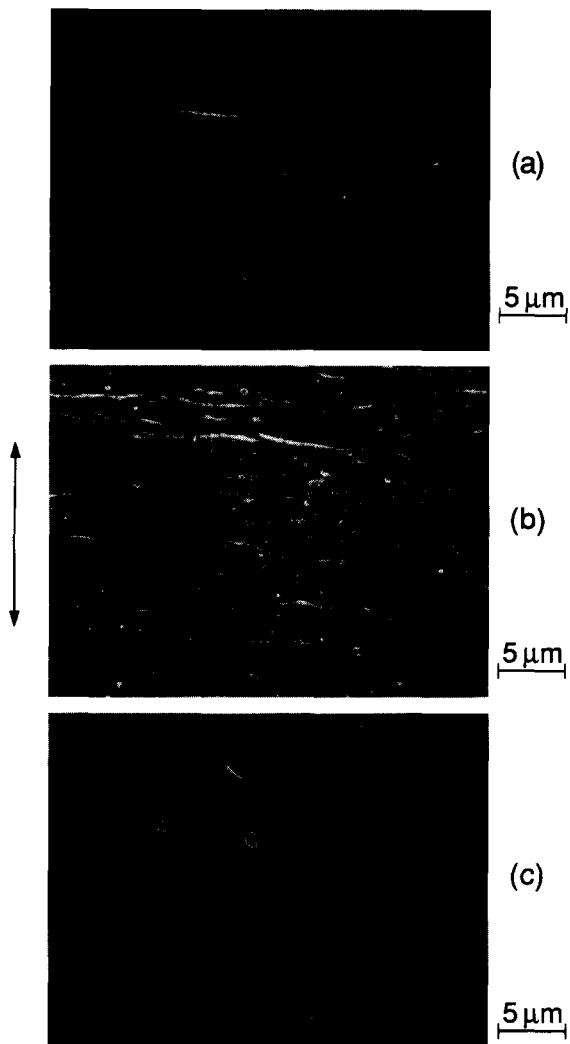


Figure 4 SEM micrographs of surface damage of SAN alloy containing 300 nm rubber particles with different rubber content. (a) Homo SAN; (b) 5 wt%; (c) 20 wt%

rubber particle site on the surface acts as a defect for initiation of crazes at low rubber content.

By contrast to the result of critical stress, the critical strain did not decrease much at low rubber content (Figure 5). The increase of critical strain at high rubber content was also higher in large particles than in small particles. Up to now, in the study of ESC of rubber-modified polymers critical strain has been suggested^{4,26} as a critical value for craze or crack formation, instead of critical stress. This approach seems to have some limitations in considering rubber effect in ESC, because the modulus of a polymer alloy is reduced when rubber is added, and then the matrix polymer experiences lower stress in the same straining condition compared with neat polymer. Thus the critical strain was not much reduced, but the critical stress decreased further with addition of rubber particles. Therefore, the effect of rubber inclusion in ESC should be studied in a view of critical stress together with critical strain.

From the morphological observation, as already seen in Figure 2, the transition of damage shape from well-developed single or two damage lines to diffuse damage lines seems to be the main reason for the increase of the critical stress at 20 wt% inclusion, since the stress should be higher to induce the diffused damage band rather than a narrow single damage line.

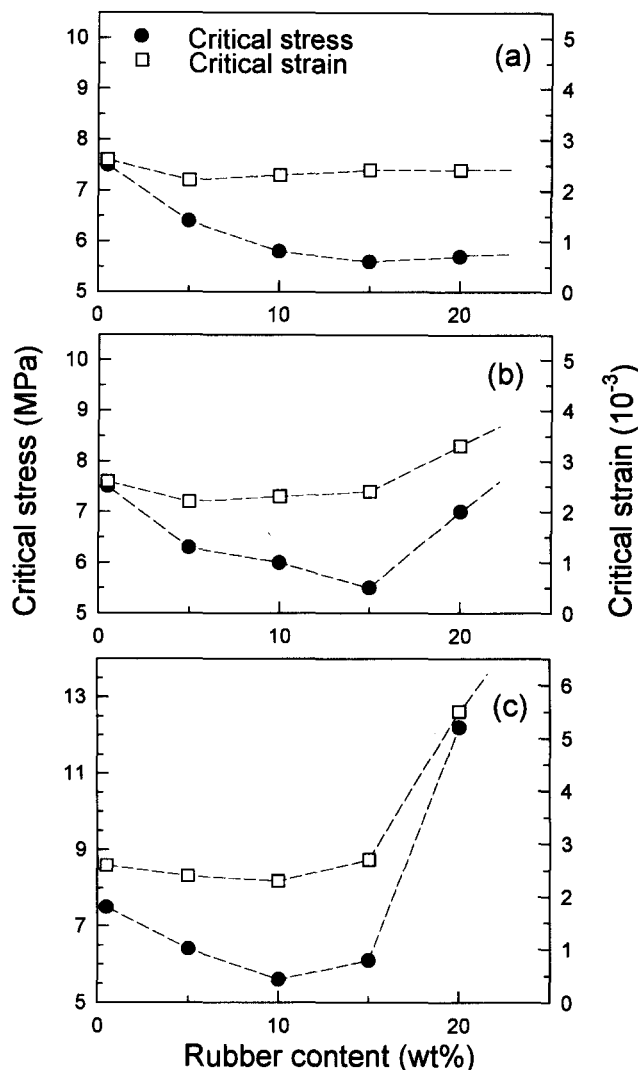


Figure 5 Critical stress and strain as a function of rubber content for PS alloy containing PBA rubber particles with different rubbery core sizes. (a) 300 nm; (b) 600 nm; (c) 1 μm

Critical stress and strain of SAN alloys

In the case of SAN alloys, the critical stress measurement with rubber content was not possible above 10 wt%, unlike PS alloys, because the craze or other damage was not detected in optical microscopic observation until the applied stress reached breaking stress of the relevant SAN alloys in air. Therefore, the experimental result for critical values were obtained only for 5 wt% rubber content and the critical values are plotted against rubber particle size (Figure 7). The critical stress shows a maximum around 300 nm. The effect of inclusion of rubber particles on ESC for PS and SAN alloys will be discussed further in the following relaxation results.

Stress relaxation of PS alloys

In the critical stress measurement the mechanical failure with time was not examined. Therefore, in order to study the mechanical failure with time the stress relaxation experiment in the Freon environment was performed. To compare the stress relaxation behaviour in the air and in the Freon environment, Freon vapour is exposed to the specimen after loading for 1 min in the air. As can be seen in Figure 8, the stress relaxed very rapidly with time right after Freon exposure. The relaxation rate

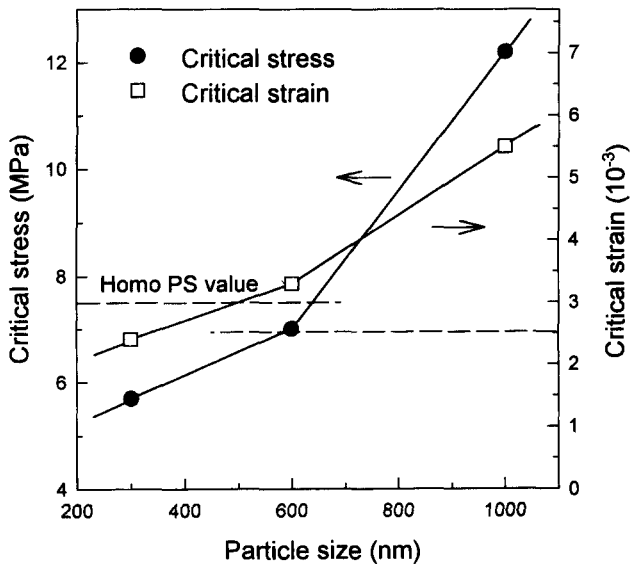


Figure 6 Critical stress and strain as a function of rubbery core size for PS alloy containing 20 wt% of PBA rubber particles

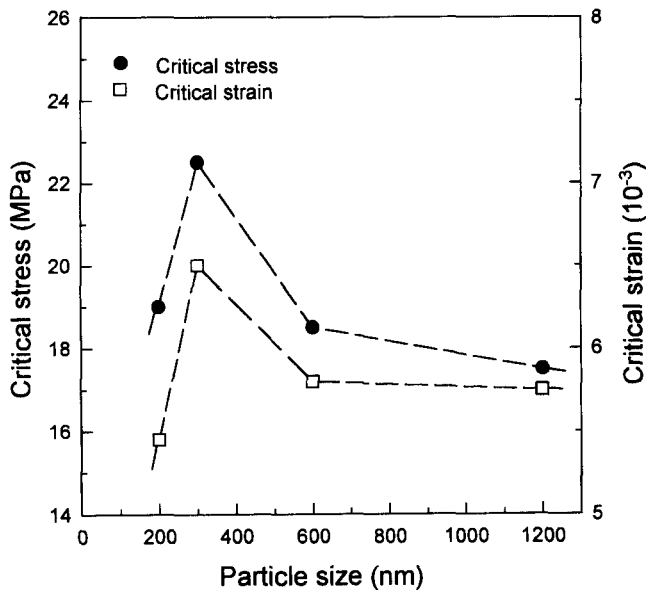


Figure 7 Critical stress and critical strain of SAN alloy containing 5 wt% PBA rubber particles. (Particle size represents the diameter of the rubbery core)

in the air was rather slow, and it was almost negligible compared with the relaxation rate in Freon vapour for the experimental time scale for all polymer alloys, irrespective of particle size and rubber content. Therefore the relaxation behaviour of PS or SAN alloys in a Freon environment can be compared without considering relaxation in the air.

The stress relaxation curves of PS alloy with different rubber content after exposure of Freon vapour are shown in Figures 9a and 9b for 300 nm and 2 μm rubber particles, respectively. The imposed stress level for all PS alloys was fixed at 9.8 MPa, which is higher than critical ESC stress of homo PS in Freon vapour. The trend of stress relaxation with particle size is almost the same with critical stress results as already shown in Figures 5 and 6. For small size particles such as 300 nm particles only

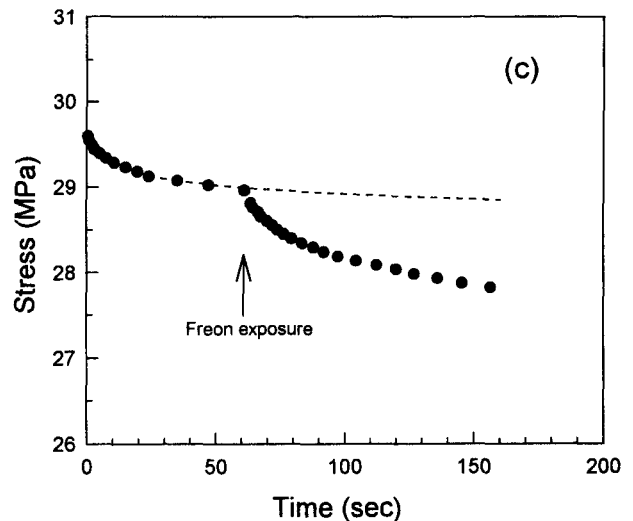
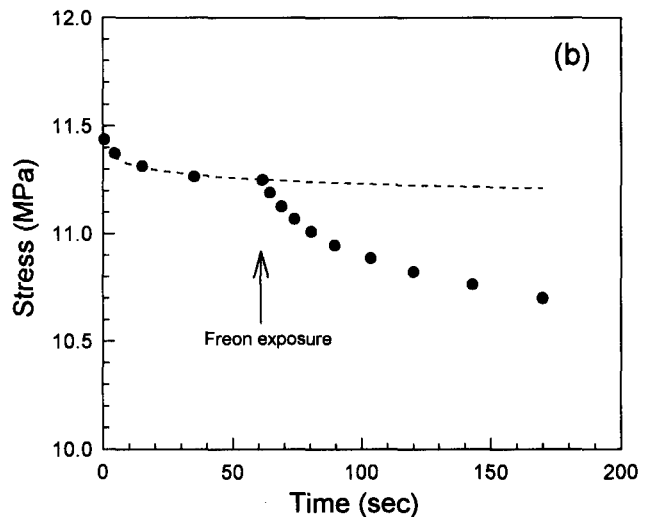
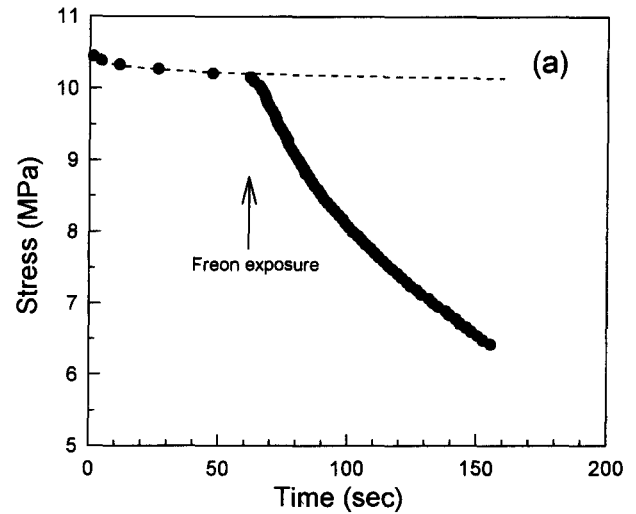


Figure 8 Relaxation behaviour of styrenic polymers in Freon vapour. (a) Homo PS; (b) PS containing 20 wt% of 1 μm PBA rubber particles; (c) SAN containing 20 wt% of 300 nm PBA rubber particles. Dotted line represents relaxation curve of relevant polymers in the air

20 wt% rubber content showed a slight improvement in stress relaxation behaviour in Freon vapour (Figure 9a), whereas large size particles such as 2 μm showed much improvement in resistance above 15 wt% inclusion (Figure 9b).

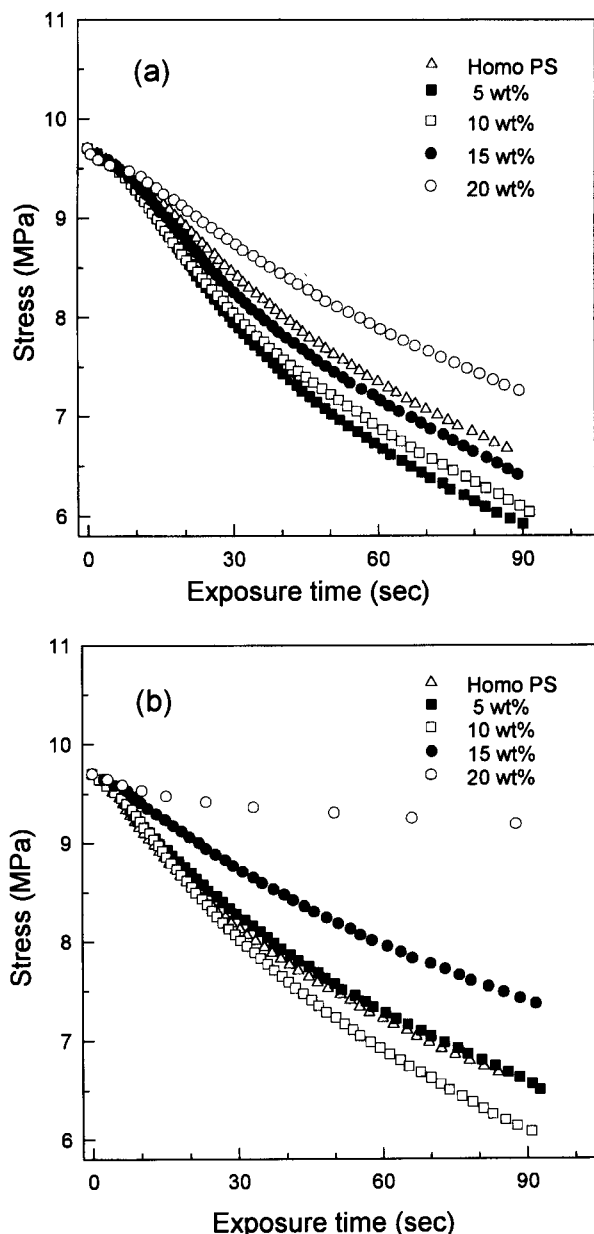


Figure 9 Stress relaxation of PS alloy after Freon exposure with different rubber content. (a) 300 nm; (b) 2 μm rubber particles

The effect of particle size can be clearly seen for 20 wt% inclusion (Figure 10). In Freon vapour environment, the stress relaxes rapidly in the case of small particle inclusions, whereas for the inclusion of large particles above 1 μm the stress does not relax much with time. From this result it is inferred that large particles of 1–2 μm are large enough to improve the ESC resistance to Freon vapour for PS alloys.

In the stress relaxation process for PS alloys of low rubber content, the developed craze on the surface of specimen penetrated into bulk very rapidly with time to an appreciable depth, right after exposure of Freon vapour (Figure 3a), which caused the rapid relaxation of the stress. This is due to the successive penetration of Freon molecules from the surface of the specimen to the craze tip through the voids of developed crazes. However, with increase of rubber content, especially in large particles, the damage was limited near the surface region, and the damage becomes small pre-mature craze bundles with no void in the broad region (Figure 3c).

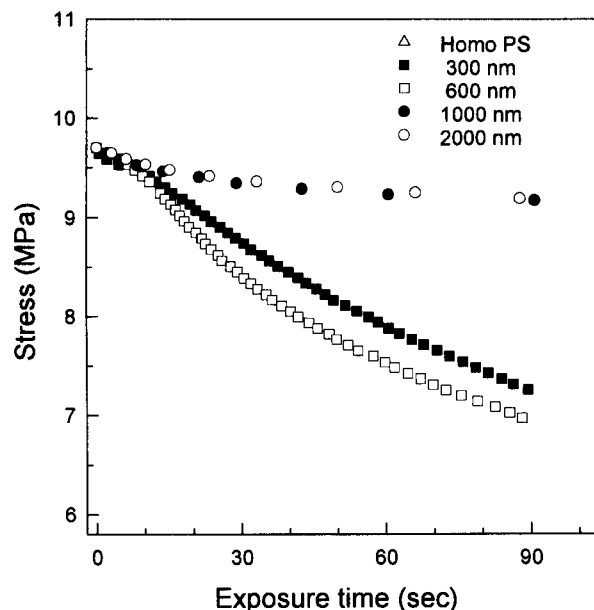


Figure 10 Stress relaxation of PS alloy containing 20 wt% PBA rubber content with different particle sizes after Freon exposure

Moreover the craze does not penetrate into the bulk side, which results in a slow relaxation rate. Considering the permeation process of Freon molecules, Freon molecules need a long time to permeate into the bulk through the dense structure of pre-mature craze bundles, rather than well developed craze structure with many voids, which affects the relaxation rate of PS alloy, i.e. the stress relaxation rate for homo PS or PS alloy with a low content of small particles is much faster than that for PS alloy containing large particles.

Stress relaxation of SAN alloys

The stress relaxation behaviour of SAN alloy in Freon vapour shows quite different results from that of PS alloy in aspect of rubber particle size. For SAN alloys, inclusion of about 300 nm particles shows the best resistance to Freon vapour, but inclusion of large size particles did not show good resistance (Figures 11 and 12). Moreover the relaxation rate is sensitive to the content of rubber particles. The relaxation rate for low rubber content was faster than that for homo SAN, like PS alloy, which suggests that small amount of included rubber particles becomes stress concentration points and induce damage lines rather than suppressing the development of damage. In the microscopic observations, the damage lines were initiated at the rubber inclusion site of the surface. The stress relaxation results of SAN alloys shown in Figures 11 and 12 also implies that the improvement of ESC by rubber modification needs some amount of rubber, as already shown in the result of critical stresses of PS alloys.

In the case of SAN, the retardation of stress relaxation by rubber inclusion is also attributed to the change in shape of damage lines on the specimen surface, i.e. the damage lines gradually disappeared with the increase of rubber content (Figure 4). Consequently, the retardation of stress relaxation by rubber inclusion is mainly due to the difficulty of penetration of the damage into bulk, which is related to the permeation of Freon molecules to the craze tip.

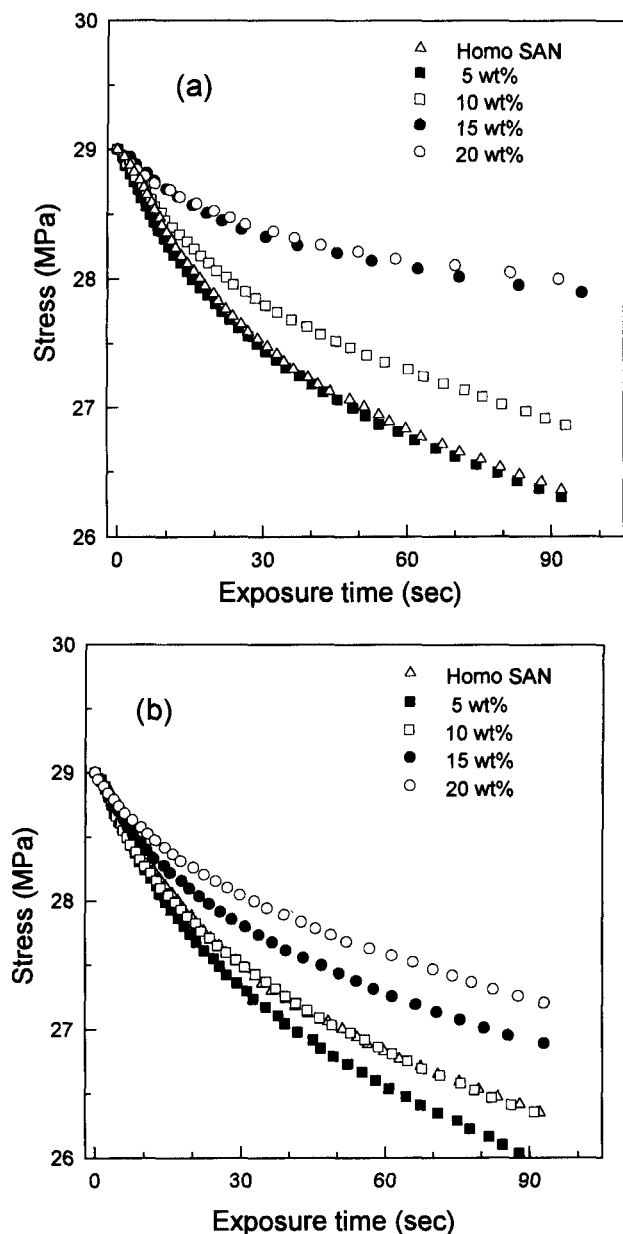


Figure 11 Stress relaxation of SAN alloy after Freon exposure with different rubber content. (a) 200 nm; (b) 1.2 μm PBA rubber particle

Plasticization of PS and SAN alloys

It is important to know how much of the T_g s of the alloys are reduced by the Freon vapour and how the rubber particles affect that, since it has been known that the critical strain for craze initiation in an ESC experiment is closely related with the depression of T_g by plasticization³. The critical strain, generally, becomes a lower value as the T_g of the plasticized part decreases in ESC of glassy polymers.

The $\tan \delta$ of plasticized homoPS was -30°C , measured by dynamic mechanical measurements. The T_g of the rubber particle decreased a little by absorption of Freon vapour. The T_g of matrix PS in a plasticized state was not much influenced by the incorporation of rubber particles. Considering that the depression of a matrix's T_g is mainly determined by the interaction between the matrix polymer itself and the ESC agent, the result does not seem to be strange. From these results, it was confirmed that the increase of critical stress by the addition of

rubber particles as already shown in Figure 4 is not related to the T_g variation of the plasticized region of the matrix itself. Therefore, the increase of critical stress may be related to the change of deformation mode as already shown in the micrographs (Figures 2 and 3).

The plasticization effect in SAN alloy was also observed in morphological observations, but the T_g of the plasticized part was hard to detect, because the degree of plasticization was very small in Freon vapour, i.e. the specimen surface was still rigid at room temperature after a long time exposure. It is presumed that the T_g of plasticized part is somewhat above room temperature. More work is needed to study the plasticization effect on SAN alloys.

Rubber particle size effect

In this experiment, the effect of rubber particle size on critical stress (Figures 6 and 7) and stress relaxation behaviour (Figures 10 and 12) was nearly the same as that for the toughening behaviour of PS or SAN, i.e. the optimum rubber particle size for toughening of PS and SAN is known to be around $2\mu\text{m}$ and $0.3\mu\text{m}$, respectively³³⁻³⁶.

In toughening of PS by rubber particles, rubber particles below $1\mu\text{m}$ are not very effective in developing multiple crazing, which is known to be the main toughening mechanism of rubber-modified PS^{35,36}. Therefore, there is some similarity of particle size effect in inert and in aggressive fracture modes. The important feature is that the large rubber particles suppress craze development rather than initiation of crazes in this environmental condition, i.e. higher critical stress was needed to develop craze bundles over the broad surface at high rubber content.

Considering the inert fracture behaviour of ABS resin in aspect of particle size, the fracture toughness of rubber modified SAN alloys shows maximum toughness around 300-nm particles^{33,34}. In the deformation of ABS in inert conditions, small particles are prone to induce shear deformation and large particles above $1\mu\text{m}$ are likely to induce crazing^{33,37}. However, considering the ESC damage developed on the specimen surface, it is not proper to apply the deformation mechanism of inert conditions to these ESC phenomena. In the case of SAN alloys, it seems that the improvement of fracture resistance in Freon vapour by the incorporation of rubber particles is induction of diffuse surface damage over the specimen surface, instead of localized damage like crazes or cracks.

It is presumed that the particle size effect in the ESC of styrenic polymer alloys depends on the deformation mode of matrix in Freon vapour, i.e. crazing or shear yielding. For homo PS, the deformation mode by Freon vapour was crazing. To prevent craze propagation the particle size must be large enough to bridge the developed craze, so large particles are effective on this viewpoint. In microscopic examination, it was observed that the large rubber particles hinder craze growth by bridging the cleavage (Figure 13b). But small particles did not bridge the large size craze. Instead, small size particles are sometimes observed inside the craze fibril (Figure 13a). From these morphological observations, for PS alloys large particles seem to be more effective to depress the initiation and propagation of craze in Freon vapour, since the size of rubber particles was larger than the thickness of dry-craze by nearly one or two orders.

In the case of SAN, the deformation mode in Freon vapour was a yielded line, so the effect of bridging a cleavage by large rubber particles cannot be applied to this ESC deformation. At the moment, a reasonable explanation for the particle size effect is not possible. However, considering small particles such as $0.3\ \mu\text{m}$ were more effective in ESC resistance than large particles (Figure 7), it is speculated that the thickness of the damage line is influenced by the particle size, because the site of rubber particles on the surface is the initiation point of damage line. The other speculation is that the inclusion of a large number of small particles can effectively distribute applied stress evenly on the surface, in contrast to the inclusion of a relatively small number of large particles when the rubber content is fixed. However, the particle size effect is not clear in this environmental cracking.

Role of rubber particles

Addition of rubber particles alters the stress states in the neighbourhood of rubber particles when the specimen is stressed. This alteration affects the deformation behaviour, i.e. the balance between the tendencies of the matrix to craze or to undergo shear flow. In addition, the stress state on the surface of the specimen is also greatly altered by the Freon absorption of the rubber particles.

Considering the absorption behaviour of poly(butyl acrylate) rubber itself, the amount of Freon absorbed for 200 min was $2.7 \times 10^{-4}\ \text{g mm}^{-2}$ for homo PS and $3.1 \times 10^{-4}\ \text{g mm}^{-2}$ for 10 wt% rubber modified PS alloy in our experimental conditions. This is attributed to the polar interaction between Freon 11 and butyl acrylate³⁸. Furthermore, the rubbery poly(butyl acrylate) has more free volume and mobile chains than glassy PS, which facilitates the diffusion of small molecules. Therefore, Freon molecules diffuse in the rubber particles more rapidly than the matrix PS. In the case of SAN alloys, the amount of Freon absorbed was negligible, even though the exposure time is long enough, since SAN itself has little interaction with Freon 11. Thus, the Freon vapour only attacks the rubber particles on the surface. Therefore, it is inferred that the surface of the specimen can be easily plasticized by Freon molecules with increase of rubber content.

Comparing the relaxation curves of homo PS and PS alloys, the relaxation rate of homo PS was not changed much after Freon exposure below the critical stress. However, above the critical stress of homo PS, the relaxation rate was increased rapidly after Freon exposure. Therefore, the increase of relaxation rate in homo PS was attributed to craze development on the specimen surface. At a high rubber content ($> 15\ \text{wt}\%$), even though the applied stress was below the critical stress, a clear increase of relaxation rate was observed after Freon exposure. However, no clear damage line was developed in that case (Figure 8b). Microscopic observation reveals that the damage lines were vague and diffuse on the surface for large particle inclusions. This experimental observation assisted the enhancement of surface softening on the surface of stressed specimen by Freon absorption of rubber particles, rather than developing cracking.

In the case of SAN alloys, the critical stress could not be measured for high rubber content specimens, say 10 wt%, since it was hard to detect damage lines, although the applied stress was near to fracture stress in inert condition. However, the stress relaxed very

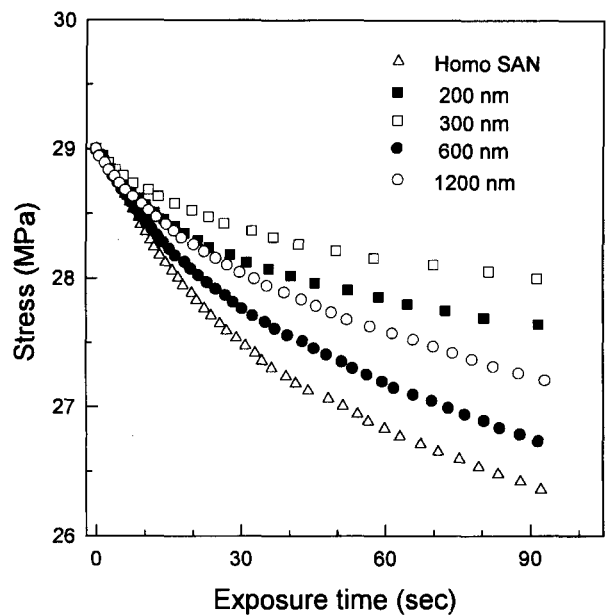


Figure 12 Stress relaxation of SAN alloy containing 20 wt% PBA rubber content with different particle sizes after Freon exposure

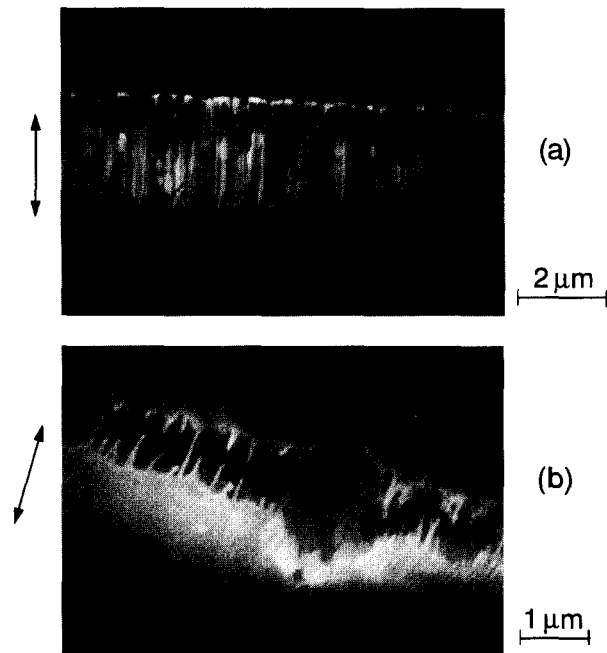


Figure 13 Craze structure of rubber-modified PS alloy containing (a) 300 nm and (b) $2\ \mu\text{m}$ PBA particles (10 wt% rubber content)

rapidly after Freon exposure, even though there are no visible damage lines on the specimen surface (Figure 8c).

Based on the experimental results, it is suggested that two processes, i.e. cracking and surface softening, compete with each other when an ESC agent contacts the surface of a stressed specimen. At higher rubber content, rubber particles on the specimen surface enhance surface softening due to Freon absorption rather than inducing local damage such as craze or deformed band. However, the polymer alloy with low rubber content does not exhibit ESC resistance because the rubber inclusion site acts mainly as an initiation point of local damage.

It is concluded, therefore, that the role of rubber

particles is to suppress the development of local deformation and enhance surface plasticization over the surface. The concept of surface plasticization was also mentioned by Imai and Brown²⁰ in their work on polycarbonate in a CO₂ gas environment. They insisted that the general yielding which is produced by plasticization of the polymer surface by the environment would inhibit the growth of crazes. In our experiment the rubber particles also enhance plasticization of the polymer surface, which results in inhibition of the growth of damage lines and reduction of surface stress.

This paper mainly focused on the effect of rubber particle size and content. The diffusion process of environmental agent and the physical properties of rubber particles, such as degree of crosslinking and chemical composition are also important parameters for the ESC resistance of styrenic polymer alloys. Further systematic experiments are needed to address these questions.

CONCLUSIONS

The addition of rubber particles to styrenic polymers improves the environmental stress cracking resistance in Freon vapour. But at low rubber content, the rubber particle site behaves as a defect and causes surface damage easily. However, above 15 wt% rubber content the critical stress increases with increasing rubber content.

For PS alloys, the larger particles above 1 μm were more effective for the ESC resistance than the smaller particles. The larger particles were found to prevent the craze formation more effectively due to enhanced surface plasticization, and hinder craze growth by bridging the crazes. The surface damage was changed from a well-structured single craze line to a flock of small size crazes over a broad surface with increasing rubber content.

For SAN alloys, the rubber particles of around 300 nm were the most effective for the ESC resistance. The surface damage of SAN was a yielded line but the damage line becomes vague over the surface with increasing rubber content. From the above results, it is presumed that the role of rubber particles in ESC is to promote surface plasticization and to suppress local deformation on the surface of the specimen.

ACKNOWLEDGEMENTS

This work was supported by a research grant from the Ministry of Education Research Funds for Advanced Materials, 1995 and the Engineering Research Center for Functional Polymers, which is funded by the Korea Science and Engineering Foundation. Additional

support of this research by a research fellowship from Sudang Foundation is also gratefully acknowledged. MSL thanks the Hanwha Chemical Corporation for the Ph.D. Studentship.

REFERENCES

1. Kambour, R. P., *J. Polym. Sci., Macromol. Rev.*, 1973, **7**, 1.
2. Bernier, G. A. and Kambour, R. P., *Macromolecules*, 1968, **1**, 393.
3. Kambour, R. P., Romagosa, E. E. and Gruner, C. J., *Macromolecules*, 1972, **5**, 335.
4. Faulkner, D. L., *Polym. Eng. Sci.*, 1984, **24**, 1174.
5. Kawagoe, M. and Kitagawa, M., *J. Materials Sci.*, 1987, **22**, 3000.
6. Vincent, P. I. and Raha, S., *Polymer*, 1972, **13**, 183.
7. Narisawa, I., *J. Polym. Sci., A-2*, 1972, **10**, 1789.
8. Andrews, E. H. and Bevan, L., *Polymer*, 1972, **13**, 337.
9. Williams, J. G. and Marshall, G. P., *Proc. R. Soc. Lond., A*, 1975, **342**, 55.
10. Mai, Y. W., *J. Mater. Sci.*, 1976, **11**, 303.
11. Kramer, E. J. and Bubeck, R. A., *J. Polym. Sci. Polym. Phys. Ed.*, 1978, **16**, 1195.
12. Kramer, E. J., Krenz, H. G. and Ast, D. G., *J. Polym. Sci. Polym. Phys. Ed.*, 1978, **16**, 349.
13. Bubeck, R. A., Arends, C. B., Hall, E. L. and Vander Sande, J. B., *Polym. Eng. Sci.*, 1981, **21**, 624.
14. Wyzgoski, M. G. and Novak, G. E., *J. Mater. Sci.*, 1987, **22**, 2615.
15. Nielsen, L. E., *J. Appl. Polym. Sci.*, 1959, **1**, 24.
16. Gent, A. N. and Hirakawa, H., *J. Polym. Sci., A-2*, 1968, **6**, 1481.
17. Schirrer, R. and Galleron, G., *Polymer*, 1988, **29**, 634.
18. Breen, J. and Van Dijk, D. J., *J. Mater. Sci.*, 1991, **26**, 5212.
19. Olf, H. G. and Peterlin, A., *J. Polym. Sci. Polym. Phys. Ed.*, 1974, **12**, 2209.
20. Imai, Y. and Brown, N., *Polymer*, 1977, **18**, 298.
21. Brown, N. and Metzger, B. D., *J. Polym. Sci., Polym. Phys. Ed.*, 1980, **18**, 1979.
22. Brown, N., *Macromol. Sci. -Phys.*, 1981, **B19**(3), 387.
23. Wu, J. C. B. and Brown, N., *J. Mater. Sci.*, 1982, **17**, 1311.
24. Brown, N. and Fischer, S., *J. Polym. Sci., Polym. Phys. Ed.*, 1975, **13**, 1315.
25. Kefalas, V. A. and Argon, A. S., *J. Mater. Sci.*, 1988, **23**, 253.
26. Henry, L. F., *Polym. Eng. Sci.*, 1974, **14**, 167.
27. Savadori, A., Bacci, D. and Marega, C., *Polymer Testing*, 1987, **7**, 59.
28. Cho, K. and Lee, M. S., *Polymer*, in press.
29. Miller, P. and Kramer, E. J., *J. Mater. Sci.*, 1990, **25**, 1751.
30. Hoa, S. V., *Polym. Eng. Sci.*, 1980, **20**, 1157.
31. Cook, D. G., Rudin, A. and Plumtree, A., *J. Appl. Polym. Sci.*, 1992, **46**, 1387.
32. Krause, S., in *Polymer Blends*, Vol. 1, ed. D. R. Paul and S. Newman. Academic Press, New York, 1978, p. 35.
33. Donald, A. M. and Kramer, E. J., *J. Mater. Sci.*, 1982, **17**, 1765.
34. Echte, A., in *Rubber-Toughened Plastics*, ed. C. K. Riew. American Chemical Society, Washington DC, 1989, p. 46.
35. Bucknall, C. B. and Smith, R. R., *Polymer*, 1965, **6**, 437.
36. Kambour, R. P., *Nature*, 1962, **195**, 1299.
37. Hagerman, E. M., *J. Appl. Polym. Sci.*, 1973, **17**, 2203.
38. Brandrup, J. and Immergut, E. H. (ed.), *Polymer Handbook*, 3rd edn. Wiley-Interscience, New York, pp. VII-519.